Research Article | Vol. 25, No. 17 | 21 Aug 2017 | OPTICS EXPRESS 19672
Optics EXPRESS

Single mode fiber based delivery of OAM light by 3D direct laser writing

KSENIA WEBER,[1] FELIX HÜTT,[1] SIMON THIELE,[2] TIMO GISSIBL,[1] ALOIS HERKOMMER,[2] AND HARALD GIESSEN[1,*]

[1]*4th Physics Institute and Research Center SCoPE, University of Stuttgart, Pfaffenwaldring 57, 70569 Stuttgart, Germany*
[2]*Institute for Applied Optics and Research Center SCoPE, University of Stuttgart, Pfaffenwaldring 9, 70569 Stuttgart, Germany*
**h.giessen@pi4.uni-stuttgart.de*

Abstract: We demonstrate orbital-angular momentum (OAM) light up to a topological charge of $l = 3$ behind a single mode fiber. Femtosecond 3D direct laser writing is used to fabricate spiral phase plates of $l = 1, 2$ and 3, composed of 10 discrete steps, on the tip of single mode optical fibers. These structures efficiently convert out-coupled light from the fiber at 785 nm wavelength into optical vortex beams carrying an orbital-angular momentum of $l\hbar$ per photon. Far field intensity patterns and interferograms of the OAM beams are recorded using a CCD camera. The results are in excellent agreement with numerical simulations obtained from the wave propagation method.

OCIS codes: (050.4865) Optical vortices; (060.2430) Fibers, single-mode; (110.6895) Three-dimensional lithography; (120.5060) Phase modulation; (220.4000) Microstructure fabrication.

References and links

1. L. Allen, M. W. Beijersbergen, R. J. C. Spreeuw, and J. P. Woerdman, "Orbital angular momentum of light and the transformation of Laguerre-Gaussian laser modes," Phys. Rev. A **45**(11), 8185–8189 (1992).
2. M. Padgett, J. Courtial, and L. Allen, "Light's orbital angular momentum," Phys. Today **57**(5), 35–40 (2004).
3. J. Leach, J. Courtial, K. Skeldon, S. M. Barnett, S. Franke-Arnold, and M. J. Padgett, "Interferometric methods to measure orbital and spin, or the total angular momentum of a single photon," Phys. Rev. Lett. **92**(1), 013601 (2004).
4. D. Bouwmeester, A. Ekert, and A. Zeilinger, *The Physics of Quantum Information* (Springer, 2000).
5. S. Haroche and J.-M. Raimond, *Exploring the Quantum: Atoms, Cavities, and Photons* (Oxford University Press, 2006).
6. A. Mair, A. Vaziri, G. Weihs, and A. Zeilinger, "Entanglement of the orbital angular momentum states of photons," Nature **412**(6844), 313–316 (2001).
7. D. G. Grier, "A revolution in optical manipulation," Nature **424**(6950), 810–816 (2003).
8. H. He, M. E. J. Friese, N. R. Heckenberg, and H. Rubinsztein-Dunlop, "Direct observation of transfer of angular momentum to absorptive particles from a laser beam with a phase singularity," Phys. Rev. Lett. **75**(5), 826–829 (1995).
9. K. Dholakia, M. MacDonald, and G. Spalding, "Optical tweezers: the next generation," Phys. World **15**(10), 31–35 (2002).
10. F. Tamburini, G. Anzolin, G. Umbriaco, A. Bianchini, and C. Barbieri, "Overcoming the Rayleigh criterion limit with optical vortices," Phys. Rev. Lett. **97**(16), 163903 (2006).
11. M. P. J. Lavery, F. C. Speirits, S. M. Barnett, and M. J. Padgett, "Detection of a spinning object using light's orbital angular momentum," Science **341**(6145), 537–540 (2013).
12. V. D'Ambrosio, N. Spagnolo, L. Del Re, S. Slussarenko, Y. Li, L. C. Kwek, L. Marrucci, S. P. Walborn, L. Aolita, and F. Sciarrino, "Photonic polarization gears for ultra-sensitive angular measurements," Nat. Commun. **4**, 2432 (2013).
13. J. Wang, J. Yang, I. M. Fazal, N. Ahmed, Y. Yan, H. Huang, Y. Ren, Y. Yue, S. Dolinar, M. Tur, and A. E. Willner, "Orbital angular momentum multiplexing," Nat. Photonics **6**(7), 488–496 (2012).
14. A. M. Yao and M. J. Padgett, "Orbital angular momentum: origins, behavior and applications," Adv. Opt. Photonics **3**(2), 161–204 (2011).
15. J. P. Torres and L. Torner, *Twisted Photons: Applications of Light with Orbital Angular Momentum* (John Wiley & Sons, 2011).
16. N. R. Heckenberg, R. McDuff, C. P. Smith, and A. G. White, "Generation of optical phase singularities by computer-generated holograms," Opt. Lett. **17**(3), 221–223 (1992).

#291550 https://doi.org/10.1364/OE.25.019672
Journal © 2017 Received 28 Apr 2017; revised 26 Jul 2017; accepted 28 Jul 2017; published 7 Aug 2017

Optics EXPRESS

17. X. Cai, J. Wang, M. J. Strain, B. Johnson-Morris, J. Zhu, M. Sorel, J. L. O'Brien, M. G. Thompson, and S. Yu, "Integrated compact optical vortex beam emitters," Science **338**(6105), 363–366 (2012).
18. L. Marrucci, C. Manzo, and D. Paparo, "Optical spin-to-orbital angular momentum conversion in inhomogeneous anisotropic media," Phys. Rev. Lett. **96**(16), 163905 (2006).
19. E. Brasselet, N. Murazawa, H. Misawa, and S. Juodkazis, "Optical vortices from liquid crystal droplets," Phys. Rev. Lett. **103**(10), 103903 (2009).
20. Z. Zhao, J. Wang, S. Li, and A. E. Willner, "Metamaterials-based broadband generation of orbital angular momentum carrying vector beams," Opt. Lett. **38**(6), 932–934 (2013).
21. J. Zeng, X. Wang, J. Sun, A. Pandey, A. N. Cartwright, and N. M. Litchinitser, "Manipulating Complex Light with Metamaterials," Sci. Rep. **3**(1), 2826 (2013).
22. J. Sun, X. Wang, T. Xu, Z. A. Kudyshev, A. N. Cartwright, and N. M. Litchinitser, "Spinning light on the nanoscale," Nano Lett. **14**(5), 2726–2729 (2014).
23. G. K. L. Wong, M. S. Kang, H. W. Lee, F. Biancalana, C. Conti, T. Weiss, and P. S. J. Russell, "Excitation of orbital angular momentum resonances in helically twisted photonic crystal fiber," Science **337**(6093), 446–449 (2012).
24. S. Paul, V. S. Lyubopytov, M. F. Schumann, J. Cesar, A. Chipouline, M. Wegener, and F. Küppers, "Wavelength-selective orbital-angular-momentum beam generation using MEMS tunable Fabry-Perot filter," Opt. Lett. **41**(14), 3249–3252 (2016).
25. M. Malinauskas, E. Brasselet, and S. Juodkazis, "Fine structuring of integrated micro-optical components using lasers," SPIE Newsroom.
26. P. Z. Dashti, F. Alhassen, and H. P. Lee, "Observation of orbital angular momentum transfer between acoustic and optical vortices in optical fiber," Phys. Rev. Lett. **96**(4), 043604 (2006).
27. Y. Jiang, G. Ren, Y. Lian, B. Zhu, W. Jin, and S. Jian, "Tunable orbital angular momentum generation in optical fibers," Opt. Lett. **41**(15), 3535–3538 (2016).
28. R. Kumar, D. Singh Mehta, A. Sachdeva, A. Garg, P. Senthilkumaran, and C. Shakher, "Generation and detection of optical vortices using all fiber-optic system," Opt. Commun. **281**(13), 3414–3420 (2008).
29. D. McGloin, N. B. Simpson, and M. J. Padgett, "Transfer of orbital angular momentum from a stressed fiber-optic waveguide to a light beam," Appl. Opt. **37**(3), 469–472 (1998).
30. R. D. Niederriter, M. E. Siemens, J. T. Gopinath, and J. U. T. G. Opinath, "Continuously tunable orbital angular momentum generation using a polarization-maintaining fiber," Opt. Lett. **41**(14), 3213–3216 (2016).
31. Y. Yan, Y. Yue, H. Huang, J. Y. Yang, M. R. Chitgarha, N. Ahmed, M. Tur, S. J. Dolinar, and A. E. Willner, "Efficient generation and multiplexing of optical orbital angular momentum modes in a ring fiber by using multiple coherent inputs," Opt. Lett. **37**(17), 3645–3647 (2012).
32. S. Lightman, R. Gvishi, G. Hurvitz, and A. Arie, "Shaping of light beams by 3D direct laser writing on facets of nonlinear crystals," Opt. Lett. **40**(19), 4460–4463 (2015).
33. I. Weiss and D. M. Marom, "Direct 3D nanoprinting on fiber tip of collimating lens and OAM mode converter in one compound element," in *Optical Fiber Communication Conference* (2016), p. Th3E.2.
34. Z. Gan, Y. Cao, R. A. Evans, and M. Gu, "Three-dimensional deep sub-diffraction optical beam lithography with 9 nm feature size," Nat. Commun. **4**, 2061 (2013).
35. T. Gissibl, S. Thiele, A. Herkommer, and H. Giessen, "Sub-micrometre accurate free-form optics by three-dimensional printing on single-mode fibres," Nat. Commun. **7**, 11763 (2016).
36. J. K. Hohmann, M. Renner, E. H. Waller, and G. von Freymann, "Three-dimensional μ-printing: an enabling technology," Adv. Opt. Mater. **3**(11), 1488–1507 (2015).
37. T. Grossmann, S. Schleede, M. Hauser, T. Beck, M. Thiel, G. von Freymann, T. Mappes, and H. Kalt, "Direct laser writing for active and passive high-Q polymer microdisks on silicon," Opt. Express **19**(12), 11451–11456 (2011).
38. T. Gissibl, S. Thiele, A. Herkommer, and H. Giessen, "Two-photon direct laser writing of ultracompact multi-lens objectives," Nat. Photonics **10**(8), 554–560 (2016).
39. T. Gissibl, M. Schmid, and H. Giessen, "Spatial beam intensity shaping using phase masks on single-mode optical fibers fabricated by femtosecond direct laser writing," Optica **3**(4), 448–451 (2016).
40. S. Thiele, T. Gissibl, H. Giessen, and A. M. Herkommer, "Ultra-compact on-chip LED collimation optics by 3D femtosecond direct laser writing," Opt. Lett. **41**(13), 3029–3032 (2016).
41. S. Thiele, K. Arzenbacher, T. Gissibl, H. Giessen, and A. M. Herkommer, "3D-printed eagle eye: Compound microlens system for foveated imaging," Sci. Adv. **3**(2), e1602655 (2017).
42. H. P. Herzig, *Micro-Optics: Elements, Systems and Applications* (CRC, 1997).
43. S. Schmidt, T. Tiess, S. Schröter, R. Hambach, M. Jäger, H. Bartelt, A. Tünnermann, and H. Gross, "Wave-optical modeling beyond the thin-element-approximation," Opt. Express **24**(26), 30188–30200 (2016).
44. N. Radwell, R. D. Hawley, J. B. Götte, and S. Franke-Arnold, "Achromatic vector vortex beams from a glass cone," Nature Commun. **7**, 10564 (2016).

1. Introduction

Apart from the well-known spin-angular momentum of photons, which is related to circular polarization, the orbital-angular momentum (OAM) is less common. In 1992, Allen et al. recognized that certain light beams carry a quantized angular momentum and predicted that

Optics EXPRESS

each photon would contribute with a value of $L = l\hbar$ with $l = 0, \pm 1, \pm 2...$ [1]. As the complete angular momentum of any light field is composed of a spin as well as an orbital contribution, this discovery led to a better understanding of the quantized nature of light.

In particular, all beams with a helical phase front possess orbital-angular momentum which is carried by the azimuthal component of the Poynting vector [2]. The latter is expressed by the phase term $\exp(-il\theta)$ with the topological charge l and the azimuthal angle θ. As the momentum circulates around the beam axis, such beams are called vortex beams or twisted photons. A characteristic feature of OAM states is that the phase structure has a singularity at the exact center of the beam leading to zero intensity on the axis. Therefore, vortex beams exhibit a donut shaped intensity pattern. When interfering such beams with a spherical wave, spiral intensity patterns are observed. The phase characteristic of the beam is then represented by the number of spiral arms that are given by the topological charge l [3].

Owing to these properties, beams that carry OAM have attracted increased interest in recent years due to a variety of possible applications, mainly resulting from the quantized structure of the orbital momentum. The numerous applications include quantum information experiments with single photons [4–6], optical manipulation [7], as well as trapping [8] and even rotation [9] of particles. In addition, further applications have been developed comprising imaging with resolutions beyond the Rayleigh limit [10], high-precision optical measurements [11,12], and multiplexing [13]. Especially the simple fabrication process of OAM generating structures makes it highly feasible for numerous applications in biology, chemistry and physics [7,14,15].

So far, the generation of OAM beams has been demonstrated in different ways including, but not limited to, computer generated holograms [16], microscopic ring resonators [17], birefringent elements [18,19], compact metamaterials [20,21], nanowaveguides [22], helically twisted photonic cystal fibers [23], as well as spiral phase plates [24,25]. The use of spiral phase plates for the conversion of a Gaussian laser beam into an OAM-carrying beam is a particularly compact and stable method, providing a high conversion efficiency and degree of integration [24]. Unlike OAM generating metallic microstructures [20–22] which are inherently lossy, spiral phase plates are typically fabricated from transparent, dielectric materials, resulting in a high transmittance.

For many applications, simple, compact, stable, and reliable OAM light delivery is required. In this paper, we demonstrate fiber delivered OAM light by fabricating spiral phase plates on the tip of single mode fibers. In contrast to other methods, where orbital-angular momentum is generated directly inside the fiber [23,26–31], this approach offers a simple and polarization independent conversion of light without the need for specially designed fibers, external control or other additional setups. Similar experiments using 3D printed spiral phase plates which were not fiber-based, have already been conducted in the past [24,25,32]. For spiral phase plates on fiber tips however [33], up to now neither well shaped-beams, interference patterns, nor OAM generation above a topological order of $l = 1$ have been demonstrated. As the phase plates are fabricated on commercially available fibers, the method represents an easy to integrate technique for new optical communication technologies as well as other applications like optical trapping and manipulation.

The spiral phase plates are fabricated by 3D femtosecond direct laser writing, which has successfully taken additive manufacturing, also known as ‘3D printing’, to the length scales of micro- and nano-optics [34–36]. The technique is based on two-photon absorption of femtosecond laser pulses in a photoresist which is transparent at the fundamental laser wavelength. In comparison to other 3D printing approaches, it has been shown that 3D femtosecond direct laser writing is the easiest and most accurate method for the fabrication of precise and complex optical elements on the micro- and nanometer scale [35,37–41]. This

Optics EXPRESS

makes it a suitable choice for the fabrication of spiral phase plates as the process is precise, rapid, flexible, and cost-effective.

2. Design and fabrication

For a spiral phase plate of topological charge l and operating wavelength λ, the height h is given as a function of the azimuthal angle θ by

$$h(\theta) = \frac{l\theta\lambda}{2\pi(n-n_0)}; \qquad \theta \in [0, 2\pi] \tag{1}$$

where n and n_0 are the refractive indices of the phase plate material and the surrounding medium, respectively. Instead of having the height continuously depend on θ, we choose a simple spiral staircase design composed of 10 discrete steps of even height difference. The total height of each step is thus given by

$$h_m = \frac{l\lambda}{9(n-n_0)} \cdot m \tag{2}$$

with $m = 0,1,2...$ being the number of the respective step. Such a structure can very efficiently be fabricated via 3D femtosecond direct laser writing, as a much lower vertical resolution is required compared to a continuous spiral phase plate design. Thus, the number of writing layers and consequently the fabrication time is strongly reduced. We fabricate spiral phase plates of $l = 1, 2$ and 3 for an operating wavelength of $\lambda = 785$ nm from IP-Dip photoresist ($n = 1.537$) from Nanoscribe GmbH, on the tips of single mode optical fibers (SM 780HP). A schematic illustration of such a structure is shown in Fig. 1.

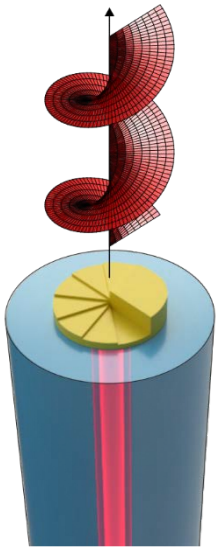

Fig. 1. Schematic illustration of the single mode fiber delivered OAM beam. Light is coupled through a single mode fiber and passes through a spiral phase plate at the fiber tip which creates a beam with a helical phase front.

The diameter of the staircase structure is chosen as 40 µm for the case of $l = 1$ and 2 and 80 µm for $l = 3$. Either way, the spiral phase plate is much larger than the single mode fiber core (Ø 4.4 µm) and the beam width of the $\lambda = 785$ nm light emitted by the laser diode (6 µm). Therefore, no influence on the OAM generation is expected. To assure good adhesion on the fiber tip, a 2 µm thick cylindrical base plate is fabricated below each spiral phase plate.

Optics EXPRESS

This design choice results in a maximum total height of well below 10 µm for all structures, ensuring low absorptive losses. The femtosecond 3D direct laser writing process is carried out using a Photonic Professional GT (Nanoscribe GmbH) system equipped with a 63x immersion objective. The fabrication relies on a dip-in approach which means that a photoresist is directly applied onto the objective lens and the tip of the approximately 10 cm long single mode fiber is immersed into it. The fiber core is then accurately centered via backside illumination and the use of the piezo stage of the Photonic Professional GT. For the subsequent 3D polymerization process, we employ the galvo-scanning technique which allows for very short fabrication times (about 3 min for an $l = 3$ spiral phase plate).

3. Simulations

The optical simulations were performed with a custom implementation of the wave propagation method which is based on scalar angular spectrum propagation. Its main advantage in the context of our stair cased spiral phase plate is that it does not rely on the thin element approximation [42] and thus correctly takes the step boundaries into account. Details about this approach can be found in [43].

Simulation parameters where chosen to closely match those of the experiment. The staircase was defined in the same way as the 3D-printed structure file with a constant refractive index of 1.537. For the input electric field, a perfect Gaussian beam with a waist of 6 µm and a wavelength of 785 nm was defined. This input field was then propagated through the structure layer by layer with 50 nm spacing in propagation direction. In lateral direction, a sampling size of 50 nm was used, which corresponds to $\lambda/16$. The interference signal was computed by coherently adding a reference beam after a propagation distance of 155 µm.

4. Results and discussion

In Fig. 2(a), an optical microscope image of an $l = 2$ spiral phase plate on the tip of a single mode fiber is shown. Backside illumination is applied in Fig. 2(b), making the fiber core visible as a bright spot in the center. The 10 individual steps of the staircase structure, as well as the precise alignment to the fiber core can clearly be identified. The quality of the SPP is further investigated via optical profilometry (Nanofocus 3D confocal microscope with a 100x objective). As visible from Fig. 2(c), the fabrication on the fiber tip was successful and the spiral phase plate exhibits no significant defects.

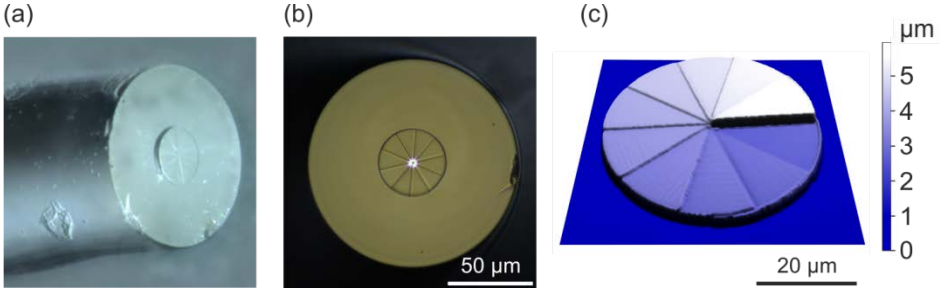

Fig. 2. Spiral phase plate composed of 10 segments with a 40 µm diameter, for $l = 2$ and 785 nm operating wavelength on the tip of a single mode optical fiber. (a) Optical micrograph. (b) Optical micrograph (top view) taken with backside illumination. (c) Optical profilometry image.

In order to characterize the light beams generated by the spiral phase plates, the single mode fibers are integrated into one arm of a Michelson interferometer and linearly polarized light from a 785 nm laser diode is coupled in from the unstructured end. Then, the far field intensity distributions of the out-coupled light are recorded. For this purpose, the reference arm of the Michelson interferometer is blocked and the out-coupled beams are imaged onto a

Optics EXPRESS

CCD chip through a 10x objective lens. It can clearly be seen in Fig. 3 that the fiber delivered light exhibits the desired donut-shaped beam profile with an optical vortex in the center. As expected from theory [1], the beam diameter increases with increasing topological charge l. These experimental results are in good agreement with the numerical simulations obtained with the wave propagation method (see Fig. 3).

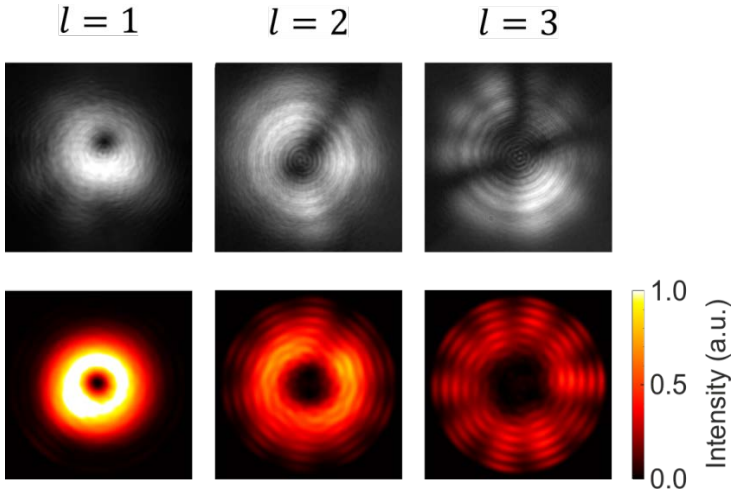

Fig. 3. Experimental (top) and simulated (bottom) far field intensity distributions of OAM beams with $l = 1, 2$ and 3, created by spiral phase plates composed of 10 segments on a single mode optical fiber.

While the measured far field intensity distributions confirm that vortex beams are created, we still have to verify that it is in fact OAM light with the correct topological charge l. In order to do so, we unblock the reference arm of the Michelson interferometer and investigate the interference pattern between the vortex beams and the Gaussian reference beam. Variable neutral density filters are used to adjust the intensity ratio between the light in both arms. To adapt the phase and optical path difference, a delay stage on a piezo crystal mounted onto a manual linear stage is set up in the reference arm. After the two beams are brought to overlap, the linear stage is shifted manually, until the optical path difference of both arms is in the range of the coherence length of the laser diode and an interference pattern is formed. The results are shown in Fig. 4. For each spiral phase plate of topological charge l, an l-fold spiral appears in the interferogram. This proves that the generation of OAM light with the desired topological charge is indeed successful. The interference patterns also show perfect agreement with those obtained from numerical simulations (see Fig. 4). Furthermore, shifting the phase of the reference beam via the piezo stage results in the expected rotation of spiral pattern which is also predicted by the simulations (see Visualization 1, Visualization 2, and Visualization 3).

Optics EXPRESS

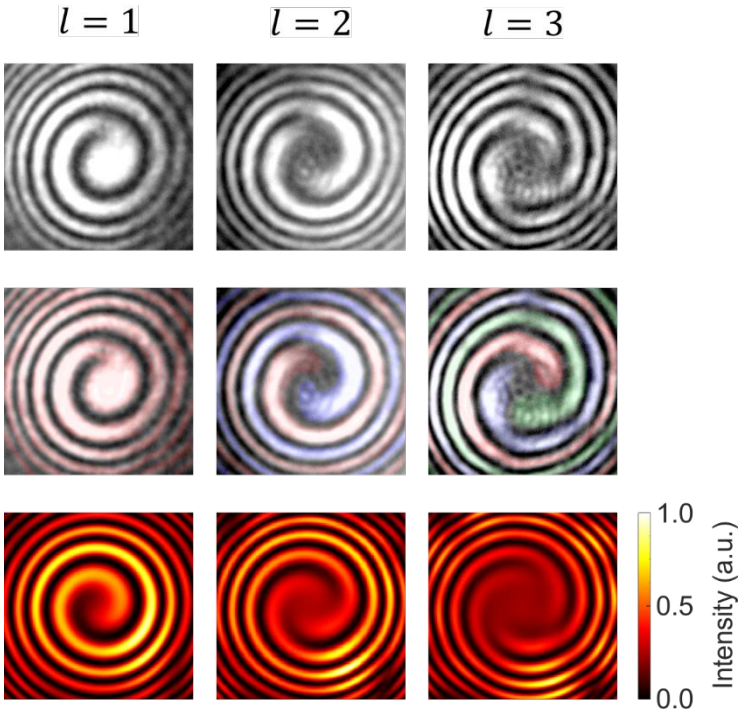

Fig. 4. Experimental (top and middle) and simulated (bottom) interferograms produced by interfering OAM beams with a Gaussian reference In the middle row, different arms of the spiral structure are highlighted by different colors to emphasize the different topological charges. .

The measured power throughput is slightly over 50% for all fibers. In reference measurements using unstructured fibers, power throughputs of 85% were achieved. This means, that about one third of the losses can be attributed to imperfect in-coupling into the single mode fibers. The remaining losses are likely due to scattering at the boundaries between the discrete steps of the phase plate. This issue was reported before when using a similar spiral phase plate design [33]. In both experiment and simulation, no influence of the spiral phase plate diameter *d* can be made out when changing from $d = 40\,\mu\text{m}$ to $d = 80\,\mu\text{m}$. The experimental results for $l = 3$ which are obtained with a $d = 80\,\mu\text{m}$ spiral phase plate are perfectly in line with the results for $l = 2$ and $l = 1$, for which a 40 µm diameter was used. The beam profiles and interference patterns for each *l* obtained from numerical simulations remain unaffected as well. This is to be expected, as in both cases, the beam width of the out-coupled light (6 µm) is much smaller than the fabricated spiral phase plate. This indicates that for both diameters the light propagating through the core only passes through a very small fraction of the spiral phase plate right in the center. For practical applications one would thus prefer a smaller spiral phase plate diameter, due to the reduced fabrication time.

5. Conclusion

In summary, we have demonstrated that orbital-angular momentum light up to a topological charge of $l = 3$ can be delivered behind a single mode optical fiber in combination with a simple spiral staircase structure fabricated via femtosecond 3D direct laser writing. The acquired far field distributions and interferograms of the orbital-angular momentum beams were found to be in excellent agreement with numerical simulations obtained by the wave propagation method. Power throughputs of over 50% were obtained for all fibers used in the experiments. Furthermore, no influence on the phase plate diameter was found for diameters

Optics EXPRESS

sufficiently larger than the beam width of out-coupled light from the single mode fiber. The simple and easy to integrate approach offers a high potential for practical applications, for example in optical trapping or manipulation. In the future, achromatic OAM beam delivery with $l = 2$ would be possible using an axicon structure [44] which is 3D printed onto the single mode fiber tip.

Funding

European Research Council (Advanced Grant COMPLEXPLAS); Deutsche Forschungsgemeinschaft (Library Fund); Bundesministerium für Bildung und Forschung (PRINTOPTICS, PRINTFUNCTION); Baden-Württemberg Stiftung (OPTERIAL).